

## A critical evaluation of the T-Scan digital occlusion analysis system

**Devaansh Bawa**

ORCID: 0009-0002-9234-5518

Main Street Children's Dentistry

7671 Quarterfield Rd Ste 400, Glen Burnie, MD 21061, USA

[bawad@iu.edu](mailto:bawad@iu.edu)**Thomas R. Katona** (Corresponding author)

ORCID: 0000-0001-9949-7237

Department of Orthodontics and Oral Facial Genetics

Indiana University School of Dentistry

1121 W. Michigan St., Indianapolis, IN 46202, USA

[tkatona@iu.edu](mailto:tkatona@iu.edu)

**Acknowledgements:** This study was supported by the Indiana University School of Dentistry (IUSD) Graduate Student Research Fund. We acknowledge the statistical assistance provided by George Eckert.

**Keywords:** Occlusion, Simulated Occlusal Forces, T-Scan, TekScan, Biomechanics

**Authors' statement:** Both authors were actively involved in all aspects of this study and the approval of the final version of the manuscript.

**Conflict of interest:** The authors have no conflicts of interest to declare.

**Funding Information:** This research did not receive any specific grant from funding agencies in the public, commercial, or not-for-profit sectors.

## A critical evaluation of the T-Scan digital occlusion analysis system

### ABSTRACT

**Background:** Universally used clinical armamentaria such as articulating paper, film, and silk, introduce an inter-dental material, thus leading to artefactual occlusal contact force measurements. Although the state-of-the-art high-tech T-Scan Novus similarly engages the dentition, the company promotes claims asserting T-Scan's ability to provide reliable measurements of contact forces and their timing.

**Aims:** A purpose of this study was to evaluate T-Scan's capability to measure occlusal contact forces and their timing. Another purpose was to examine T-Scan's data processing algorithm.

**Methods:** The forces experienced by contacting crown-crown (control) and crown-sensor-crown (T-Scan) configurations with denture teeth were measured by a load cell. For statistical purposes, 21 occlusal relationships, in 0.05 mm incremental shifts of the lower member, were tested. The load cell-measured in-occlusal plane components ( $F_x$  and  $F_y$ ) of the occlusal contact forces, for control and T-Scan, were isolated from the 5<sup>th</sup> chomp (of 7) during occlusion and disclusion when the bite force ( $F_z$ ) was 15 N and 25 N. These  $F_x$  and  $F_y$  were used to calculate  $F_{lateral}$ , the magnitude of the in-occlusal plane component of the occlusal contact force,  $F_{lateral}$ . The effects on  $F_{lateral}$  of bite force, occlusion/disclusion, and group (test/control) were analyzed using three-way repeated measures ANOVA.

**Results:** The crown-crown  $F_{lateral}$  forces are significantly ( $p < .001$ ) larger than those of crown-sensor-crown. The presence of the sensor also alters the direction of  $F_{lateral}$ . Additionally, the duration of a T-Scan chomp was about ½ seconds longer than control. Examination of the numerical algorithm reveals violations of basic engineering mechanics principles.

**Conclusion:** The T-Scan system relies on engineering mechanics (statics) calculations that use artefactual occlusal contact force magnitude measurements, approximated artefactual contact point location measurements, and assumed occlusal contact force directions. As magnitude, location and direction comprise the essential defining parameters of a force vector, just one of the 3 deficiencies, by itself, is sufficient evidence to declare the impossibility of meaningful T-Scan analyses.

## A critical evaluation of the T-Scan digital occlusion analysis system

### INTRODUCTION

Occlusal loads (forces and moments) experienced by the dentition, and the role of friction, is complex and poorly understood. This is attributable to a variety of factors including intricate contact surfaces, various material combinations (enamel-enamel, enamel-amalgam, amalgam-porcelain, etc.), and differences in lubrication (high saliva flow, xerostomia and artificial salivas). Previous studies have shown that the loads experienced by teeth are transient, complex, and counterintuitive.<sup>1, 2</sup> The same studies showed that the magnitude of the in-occlusal-plane force,  $F_{\text{lateral}}$  ( $F_{\text{lat}}$ ), in occlusion and disclusion differ, and that the maximum  $F_{\text{lat}}$  does not necessarily occur during peak bite force. The occlusion/disclusion differences can be attributed to friction.<sup>3, 4</sup>

In contrast to T-Scan (T-Scan<sup>®</sup> Novus<sup>™</sup> Sensor, Tekscan Inc., Norwood, MA, USA), the previous studies (as well as this one) measured the combined effects (*i.e.*, vector sums) of the individual occlusal contact forces. But if the vector sum of a set of individual forces is different from that of another set of forces, that means that the 2 sets must be different.

Occlusal loads have been linked to adverse clinical outcomes such as non-carious cervical lesions and implant abutment screw loosening,<sup>5-11</sup> and  $F_{\text{lat}}$  is the most destructive to the periodontium.<sup>12-15</sup> By having a better understanding of when and where contacts are made and lost, clinicians could better ameliorate deleterious occlusal contact forces with enameloplasty and occlusal equilibration. Additionally, the data could improve our conceptualization of crown-crown interactions.

T-Scan is a state-of-the-art computer-based digital occlusion analysis system. Their claims are that it can determine occlusal contact force locations, their magnitudes and their timing. However, it has been shown that the presence of an ink-based occlusal indicator paper, film or silk and, in particular, the electronic T-Scan sensor, modifies the loads experienced by the teeth.<sup>16-18</sup> Advocates of T-Scan suggest that because ink-based occlusal indicators do not measure force magnitude, T-Scan is a better option.<sup>19, 20</sup> The reliability of absolute and relative force magnitude measurements with the T-Scan sensor has been shown to be poor<sup>21</sup> while other claims are that it is capable of consistently recording and reproducing occlusal force imbalances.<sup>22</sup>

This study examined, in more detail than previously,<sup>17, 21, 22</sup> T-Scan's ability to characterize occlusal contacts. One set of critiques is a more definitive than previously published<sup>16, 21, 23</sup> scrutiny of the system's inherent hardware shortcomings. The 2<sup>nd</sup> is a heretofore unaddressed issue with T-Scan's claimed ability to time occlusal contacts. And 3<sup>rd</sup>, another unexplored area, the problematic numerical algorithm that is used to produce T-Scan's impressive, highly touted clinical displays, which viewed from an engineering perspective, violates several of the most basic tenets of engineering mechanics (statics).

## METHODS

### *Brief description*

A matching pair of 33° opposing maxillary and mandibular 1<sup>st</sup> molar denture teeth was mounted in the testing apparatus, **Figure 1A**, and set into centric occlusion. The mandibular assembly was positioned into 21 locations (including centric) in 0.05 mm increments. At each of the 21 positions, the forces acting on the lower crown were continuously measured by a load cell during 7 complete chomps of crown-crown contact and 7 with the crown-sensor-crown configuration.

### *Testing apparatus*

The apparatus (**Figure 1A**) consisted of a weighted upper assembly on two vertical precision slides (Mini-Guide, Double Carriage, Model #SEBS 9BUU2-275, Nippon Bearing Co, Ojiya, Japan). The upper assembly was cycled onto the mandibular tooth while the force ( $F_x$ ,  $F_y$ , and  $F_z$ ) components experienced by the mandibular tooth were continuously measured by a load cell (Gamma transducer SI-65-5, ATI Industrial Automation, Apex, NC, USA, **Figure 1C**). The load cell measurements were recorded via NI-DAQmx software (National Instruments Corporation, Austin, TX, USA) onto a laptop computer (Dell Inspiron 15R-5537, Dell Corporation, Round Rock, TX, USA).

### *Specimen preparation*

A pair of 33° maxillary and mandibular right first molar denture teeth (Dentsply Portrait IPN, York, PA, USA) were used. The denture teeth were trimmed to fit into cylindrical recesses within the crown holders, precision machined aluminum bars measuring 10 x 10 x 28 mm. The crown of the maxillary tooth was secured with orthodontic resin (Dentsply Caulk, Dentsply International, Milford, DE, USA) and installed in the mechanical testing machine. The mandibular tooth holder, in its holding plate, sat unclamped on the instrument's table. The cylindrical hole meant for the crown was partly filled with orthodontic resin and tack cured. The mandibular denture tooth was positioned within this resin. As the unweighted upper assembly was slowly lowered, the mandibular assembly was moved into maximum intercuspation in a Class I relationship. The resin was then allowed to cure.

### *Testing set-up*

The upper assembly with the maxillary crown was lowered onto the complete lower assembly (the load cell with the mandibular tooth components). The lower assembly was moved until the maxillary tooth fell into the Class I occlusion. This location was locked in place by clamping the load cell's base plate to the table. A carpenter's square was clamped (for the entire duration of the experiment) tightly against two 0.20 mm stainless steel shims (Feeler Stock No. 667-8, L. S. Starrett Co., Athol, MA, USA) that were sandwiched between its 2 legs and the sides of the load cell's base plate, **Figure 1**. This defined the "2020" position of centric occlusion, **Figure 2**. The position of the lower assembly was modified, in random sequence, for each of the 20 other trials by removing the shims on one or both sides, and/or replacing them with thinner or thicker ones in 0.05 mm increments.

The large T-Scan sensor (T-Scan<sup>®</sup> Novus<sup>™</sup> Sensor, Model Large #2002, Tekscan Inc., Norwood MA, USA) was used in this experiment. It was held in place with a clamp (Helping Hands,

Model #60501, 319, HFT Brand, Los Angeles CA, USA) resting on the table away from the load cell.

### *Testing*

After the lower assembly was clamped, the upper assembly was manually lowered with the MTS such that a slight slack was observed in the supporting chain. The slack ensured that the full bite force ( $F_z = \sim 28$  N) was being applied. This vertical position of the MTS actuator was set as its zero point.

At each of the 21 positions, a 14-chomp test was performed with ramp displacement control at 0.2 Hz and 4.0 mm amplitude. During the first 7 chomps, the T-Scan sensor was held in position on the mandibular tooth. Immediately after the 7<sup>th</sup> chomp, the sensor was quickly removed, and the remaining 7 chomps served as control. The shims were replaced in random order to obtain all 21 relationships, **Figure 2**. Data were uploaded as CSV files.

### *Statistical analysis*

Data was summarized by isolating the 5<sup>th</sup> chomp for test and control for each of the 21 occlusal positions. (This was done because the reliability of the T-Scan sensor improves at the 5<sup>th</sup> chomp.<sup>24-26</sup>) After isolating the 5<sup>th</sup> chomp, the values of  $F_x$  and  $F_y$  at  $F_z = 15$  N and  $F_z = 25$  N ( $\pm 0.05$  N), **Figure 1B**, in occlusion and disclusion were extracted and used to calculate  $F_{lat}$  with the Pythagorean Theorem. To reduce the possibility of errors, the  $F_x$  and  $F_y$  values were separately obtained by both authors. The effects of bite force (15 vs. 25 N), occlusion vs. disclusion, and group (test vs. control) were analyzed using three-way repeated measures ANOVA, on the ranks of the data with an unstructured variance/covariance matrix to account for correlations among observations from the same occlusal configuration and allowing different variances for each treatment combination. A two-sided 5% significance level was used for each test. Analyses were performed using SAS version 9.4 (SAS Institute, Inc., Cary, NC, USA).

### *Data normalization for graphic displays*

With the control specimens, the initial contact and the disengagement (as indicated by the bite force,  $F_z$ ) are well defined distinct points, dashed circles in **Figure 3**. Thus, the control specimen data were shifted such that its initial contact ( $0 = F_z > 0$ ) occurred at 0.5 seconds. Then, data points during the clench period (dashed box) were deleted (occasionally added) such that the total time between initial contact and disengagement (*i.e.*, the time between the dashed circles) was, arbitrarily, 1.0 second. Next, the test specimen data were shifted such that its  $F_z = 15$  N point in occlusion coincided with the corresponding  $F_z = 15$  N point of the control specimen, ●. Finally, data points were removed, or added, in the clench segment (dashed box) of the test specimen so that its data point at  $F_z = 15$  N during disclusion also overlapped, ■. All statistical analyses focused on the data values (*i.e.*,  $F_{lat}$ ) that correspond to bite forces  $F_z = 15$  N during occlusion (●) and during disclusion (■) and similarly for  $F_z = 25$  N (○ and □). Thus, for graphic purposes, all data were normalized relative to their values when  $F_z = 15$  N in occlusion and in disclusion, with the entire control chomp duration adjusted to 1 second. (Note that the statistical analyses are not affected by normalization.)

	Bite force ( $F_z$ )	
	15 N	25 N
Occlusion	●	○
Disclusion	■	□

## RESULTS

$F_{lat}$  was significantly ( $p < 0.001$ ) smaller for  $F_z = 15$  N than 25 N in all combinations. Disclusion had significantly ( $p < 0.001$ ) larger  $F_{lat}$  than occlusion, regardless of bite force or treatment group. The control group had significantly ( $p < 0.001$ ) larger  $F_{lat}$  than the T-Scan group, regardless of bite force or occlusion/disclusion.

Representative results are presented for 5 of the 21 tested configurations in **Figures 4 - 8**. As  $F_x$  and  $F_y$  are the x- and y-components of the  $F_{lat}$  vector, **Figure 1B**, the arrows drawn from the origin to a point on the curves in **Figures 4C - 8C** represent  $F_{lat}$  vectors. For example, in **Figure 4C**, as indicated by the □ at the arrow tip in the dashed circle, the arrow represents the  $F_{lat}$  vector for T-Scan in disclusion when  $F_z = 25$  N. (The symbols are in all **4C - 8C** figures, however, to reduce clutter, some arrows are not shown.)

## DISCUSSION

### *Engineering principles*

Forces and moments are classified as vector quantities (identified by bolded text) because they possess a magnitude and a direction. In addition to its magnitude and direction, to characterize a *force* vector, its line-of-action (or point of application) must also be defined. To solve a static equilibrium problem, some load (force and moment) magnitudes and/or directions and/or LOAs must be known (*i.e.*, measured, specified, or assumed), and used in the governing equilibrium equations to calculate all, or some, of the remaining unknown load magnitudes/directions/LOAs. As demonstrated, T-Scan fails in the measurement of *all* 3 characterizations of occlusal contact forces.

### *Intrinsic hardware issues*

By virtue of its presence, the T-Scan sensor converts a crown-crown contact interface into a double interfaced crown-sensor-crown contact. Due to the thickness and stiffness of the sensor, the teeth are forced into different relative positions, thereby affecting the contact locations, and possibly, the number of contact locations. And, as there is relative motion at the interfaces, the friction forces at the contacts between enamel-enamel, enamel-amalgam, resin-ceramic, etc., are replaced by friction forces at enamel-sensor/sensor-enamel, enamel-sensor/sensor-amalgam, resin-sensor/sensor-ceramic interface contacts, respectively. As a consequence, in concordance with previous studies,<sup>17, 27, 28</sup> denture crown-denture crown contacts produce larger ( $p < .001$ )  $F_{lat}$  magnitudes than denture crown-sensor-denture crown interfaces, **Figures 4 - 8**. Demonstrating

the significant differences in magnitudes is sufficient for our purposes, thus, we did not perform statistical comparisons of  $F_{lat}$  directions, although **Figures 4C – 8C** clearly show that, indeed, there are dissimilarities in directions too.

Essentially, therefore, all data obtained with the T-Scan sensor are artefactual. At best, one could argue that the data reflect the occlusion of a patient that is biting on a sensor. But even that is not true. Suppose a 3 N and a 4 N force act on the sensor at points A and B, respectively, **Figure 9A**. The equivalent force-moment system is shown in **Figure 9B**, in which the single 7 N downward force ( $= 3\text{ N} + 4\text{ N}$ ) replaces the two original downward forces. The 7 N force must be applied at C such that the 2 systems of forces produce the same moments.

Now, suppose that the same 2 forces act on the same 2 points on the sensor (*i.e.*, at A and B) as before, but the sensor is deformed, as in **Figure 9C**, and therefore the contacts are located at A' and B'. As the forces do not act parallel to each other, their resultant is 5 N in the  $36.9^\circ$  direction, the *vector* sum of the 2 forces, **Figure 9D**. The critical point is that T-Scan cannot distinguish between the configurations depicted in **Figures 9A** and in **9C**. But, as illustrated in **Figures 9B** and **9D**, their respective equivalent force systems have *nothing* in common; not their magnitudes (7 N vs. 5 N), not their directions (downward vs.  $36.9^\circ$ ), nor their lines-of-action (dashed lines). Thus, T-Scan treats these entirely different load systems identically because all it “knows” is that there is a 3 N force at a specific point *on the sensor*, A, and a 4 N force at another specific point *on the sensor* at B. It has no way of knowing where A and B are relative to each other if the sensor is deformed.

The critical importance of this observation can be explained by rotating **Figure 9C**, as in **Figure 9E**, and superimposing it on a contacting cusp, **Figure 9F**. In all drawings, the contact forces are the 3N force and the 4N force that act, respectively, on the same 2 points, A and B on the sensor. Although points A and B are always 70 mm apart on the sensor, when deformed, they are at different locations relative to each other. Thus, T-Scan cannot distinguish between the 4 distinctively different load examples depicted in **(F) – (H)**, and therefore, apparently, it treats all of them as the configuration depicted in **(A)**, *i.e.*, flat plane occlusion.

T-Scan also claims that it can assess the chronology or timing of contacts for more precise and accurate evaluation of problematic or heavy contacts. Their claim is that the sensor’s ability to measure not just occlusal contact force magnitudes, but also the timing of these forces is what gives providers more context than simple occlusal indicator papers. While true in theory, our results suggest that the system cannot determine the timing of contacts for the following reason.

To ensure that the full weight of the upper assembly was applied to the lower crown during each chomp, the travel of the hydraulic actuator of the testing machine was adjusted so that a slight slack was observed in the supporting chain when the upper assembly rested on the lower crown. The amount of that slack determined the duration of the clench period. As the slack was eyeballed, the clench duration could not be controlled. (See Thompson<sup>29</sup> for a detailed explanation.) Therefore, for graphical purposes the data had to be normalized, as described in Methods, **Figure 3**.

Although **Figure 3** is the loading profile for Centric, it is virtually identical to the other loading profiles. The critical relevant factors are the “toes” at both ends of the T-Scan graph, longer at the initial contact than at disclusion. These indicate that prior to hard contact and complete disengagement, the load cell measured the bite force it took to deform the sensor so that it conformed to the occlusal surfaces, and as the bite force was released, the load cell also measured the spring-back of the sensor.

Thus, the toes are entirely artefactual because they are introduced by the sensor, and in essence, they reflect the sensor’s mechanical properties. The toes are unaffected by the normalization of the data, but they make it impossible to identify the initial and final contacts. An estimate is that the occlusion and disclusion toes, ~0.3 sec and ~0.2 sec, respectively, add ~0.5 sec to the durations of all chomps, **Figure 3**. It is therefore difficult to accept T-Scan’s claim that it can time occlusal contacts that occur during a process (a chomp), that in their measurements is overstated by about ½ second.

#### *Numerical algorithm issues*

There are no readily available details about T-Scan’s numerical algorithms because, apparently, the methods are proprietary.<sup>30</sup> With no information to the contrary, and because practical alternatives do not exist, it must be presumed that the computations are based on basic Newtonian force and moment static equilibrium principles.

T-Scan claims to measure the individual occlusal contact force magnitudes and asserts the ability to pinpoint their contact locations (<https://www.tekscan.com/products-solutions/digital-occlusal-analysis>). These are 2 of the 3 required force vector parameters noted above. But, as described, it has been demonstrated that contact forces between occlusal surfaces and sensor do not replicate (in magnitude and direction) direct occlusal surface-occlusal surface contact forces, **Figures 4 - 8**. Furthermore, the T-Scan contacts are localized relative to its flat undeformed sensor, not relative to the actual “cuspy” terrain of the occlusal plane, **Figure 9**. Thus, the T-Scan-measured contact force locations are faulty measurements of artefactual locations.

Individual occlusal contact force direction (the 3<sup>rd</sup> essential attribute of a force vector) is rarely (if ever) mentioned in the T-Scan literature. Hence, purely by conjecture based on depictions in promotional images, the calculations may be using the assumption that the individual occlusal contact forces are perpendicular to the occlusal plane. That would be the simplest and most intuitive configuration, but unfortunately, 100% wrong with cusp incline contacts. The bottom line is that the T-scan sensor cannot provide force orientation, so for computational purposes, contact force directions must be assumed.

#### *Miscellaneous issues*

Another complication is that with the same bite force ( $F_z$ ), occlusal contact forces are smaller ( $p < .001$ ) in occlusion than in disclusion (**Figures 4B – 8B**). The exception is for T-Scan in Centric (2020), **Figure 4B**. However, Centric is somewhat aberrant because its  $F_{lat}$  values are relatively much smaller than the other configurations, and therefore, it is more affected by the presence of the sensor.



Counterintuitively, the peak values of  $F_{lat}$  do not necessarily happen when the bite force ( $F_z$ ) is maximum. For 2020 (**Figure 4B**), the peak  $F_{lat}$  T-Scan value occurs during occlusion when  $F_z = 11.3$  N. For control, it is when  $F_z = 15.9$  N in disclusion, as indicated by the  $\diamond$ . For 2520 (**Figure 6B**), the peaks occur when  $F_z = 17.2$  N and  $15.2$  N, both during disclusion. Thus, in these examples, the peak values of  $F_{lat}$  occur at much smaller values of the bite force than its maximum,  $F_z = \sim 28$  N. (Clenching may serve to reduce large damaging in-occlusal plane forces.)

It is not clear how the occlusion/disclusion discrepancy and the timing of the peak  $F_{lat}$  values affect treatment, but it is not obvious how, or if, T-Scan takes these phenomena into account.

We focused on the 5<sup>th</sup> chomp because of the understanding that it takes 4 chomps to stabilize the T-Scan readings.<sup>24-26</sup> However, our data indicate that the measurements do not necessarily stabilize even after 7 chomps, the limit set by our protocol, **Figure 10**.

Rough profilometer (ProScan 2000 2D Laser Profilometer, Scantron Industrial Products Ltd, Somerset, England) measurements show that there are  $\sim 0.01$  mm “speed bumps” spaced  $\sim 1.1$  mm apart on the surface of the sensor, **Figure 11**. And, crisscrossing at  $90^\circ$ , they are replicated on the bottom surface. Considering that the  $0.05$  mm shifts in the occlusal relationship produce significant changes in the occlusal contact forces, the  $0.02$  mm bumpiness of the sensor is probably a major impediment to the relative movements of the contacts. Thus, this surface irregularity is another contributor to the T-Scan-specific artefactual nature of their measurements.

## CONCLUSION

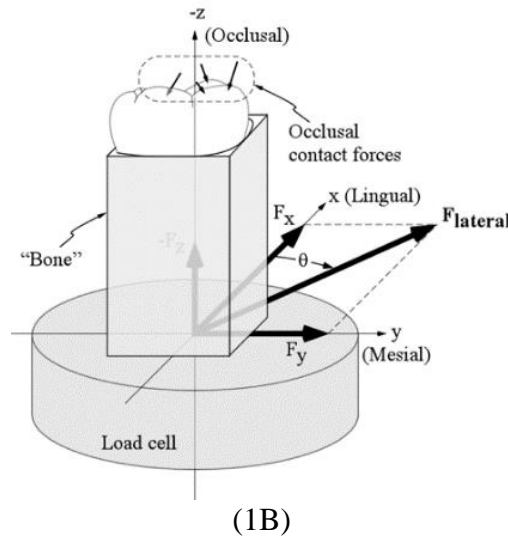
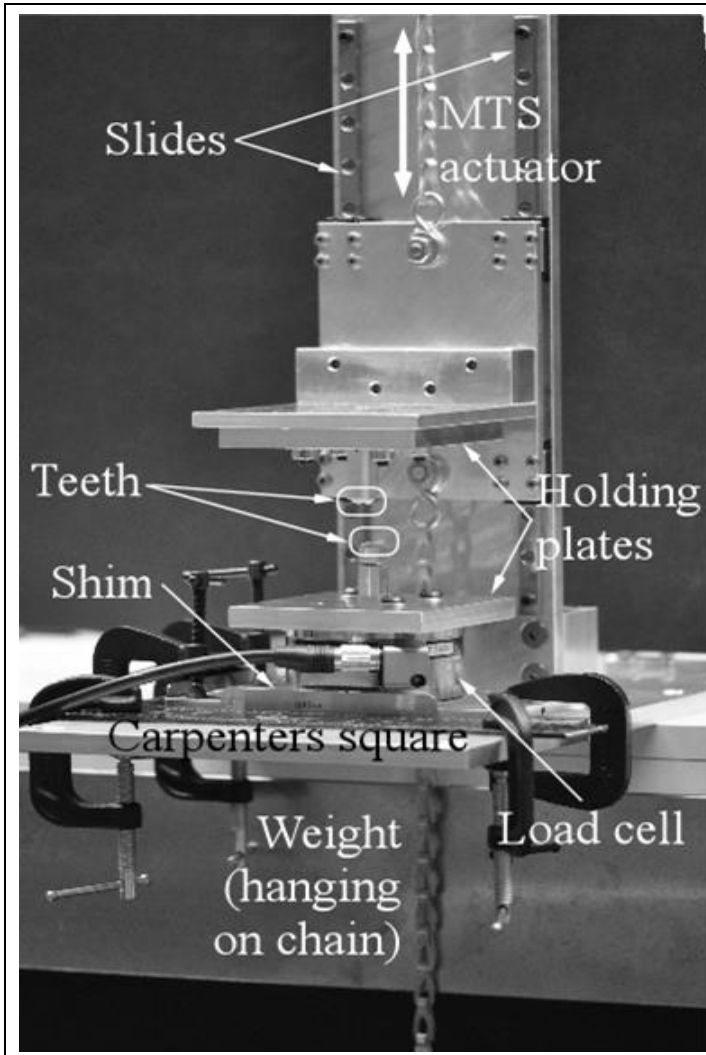
The T-Scan system relies on calculations that use artefactual occlusal contact force magnitudes, approximated artefactual contact point locations, and assumed occlusal contact force directions. According to engineering principles, just one of these 3 shortcomings, by itself, would be sufficient to invalidate all T-Scan analyses.

## REFERENCES

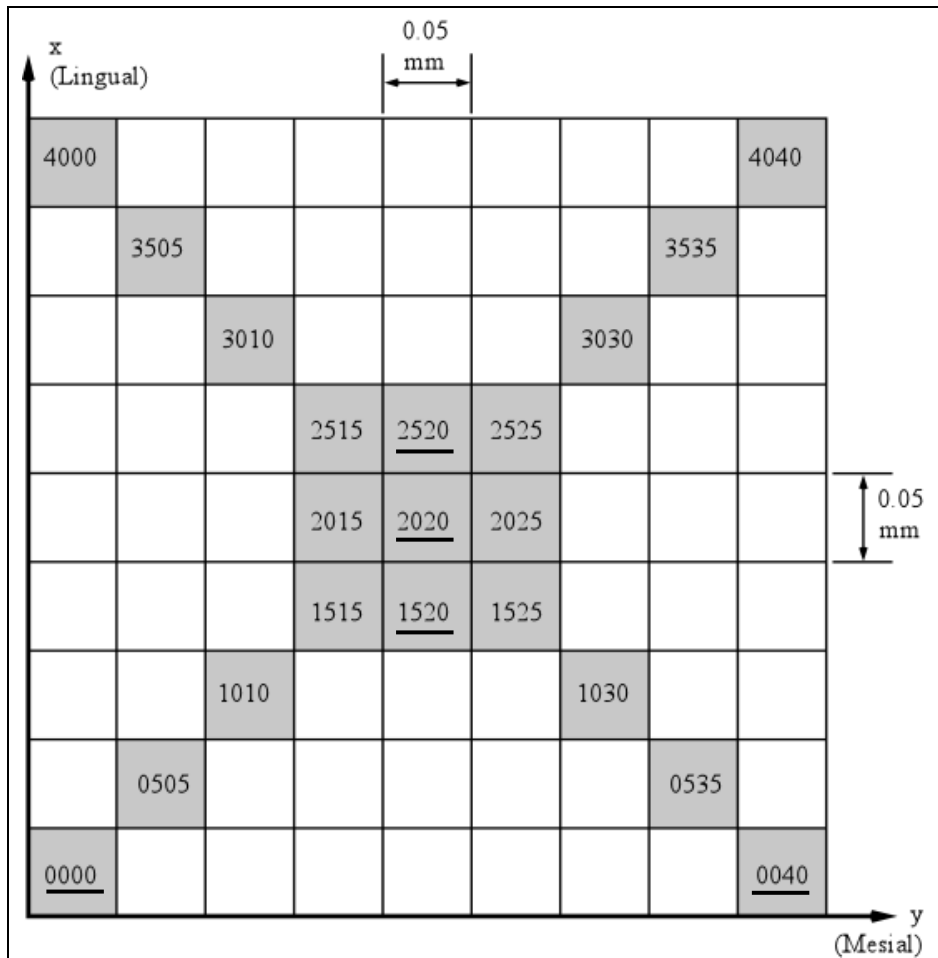
1. Katona TR, Eckert GJ. The mechanics of dental occlusion and disclusion. *Clin Biomech (Bristol, Avon)*. 2017;50:84-91. <https://doi.org/10.1016/j.clinbiomech.2017.10.009>.
2. Katona TR, Eckert GJ. The roles of wedging and friction in the mechanics of dental occlusal contacts. *IUPUI ScholarWorks*. 2019. Permanent Link: <https://hdl.handle.net/1805/30357>.
3. Katona TR. A mathematical analysis of the role of friction in occlusal trauma. *J Prosthet Dent*. 2001;86:636-643. <https://doi.org/10.1067/mpr.2001.120068>.
4. McCrea ES, Katona TR, Eckert GJ. The effects of salivas on occlusal forces. *J Oral Rehabil*. 2015;42:348-354. doi: <https://doi.org/10.1111/joor.12260>.
5. Attiah EMN, AlGendy AA, Mostafa TMN. Effect of dynamic cyclic loading on screw loosening of retightened versus new abutment screw in both narrow and standard

- implants (in-vitro study). *International Journal of Implant Dentistry*. 2020;6:30.<https://doi.org/10.1186/s40729-020-00229-3>.
6. Bustos AJ, Al-Talib T, Abubakr NH. Retrospective Analysis of the Association of Non-Carious Cervical Lesions with Bruxism. *Open Journal of Stomatology*. 2020;10:11-18. <https://doi.org/10.4236/ojst.2020.102002>.
  7. Katona TR, Eckert GJ. A proposed mechanism for non-carious cervical lesions, root resorption and abutment screw loosening. *IUPUI ScholarWorks*. 2022. Permanent Link: <https://hdl.handle.net/1805/30098>.
  8. Kolak V, Pešić D, Melih I, Lalović M, Nikitović A, Jakovljević A. Epidemiological investigation of non-carious cervical lesions and possible etiological factors. *J Clin Exp Dent*. 2018;10:e648-e656. <https://doi.org/10.4317/jced.54860>.
  9. Ommerborn MA, Schneider C, Giraki M, et al. In vivo evaluation of noncarious cervical lesions in sleep bruxism subjects. *J Prosthet Dent*. 2007;98:150-158. [https://doi.org/10.1016/s0022-3913\(07\)60048-1](https://doi.org/10.1016/s0022-3913(07)60048-1).
  10. Silva AG, Martins CC, Zina LG, et al. The association between occlusal factors and noncarious cervical lesions: a systematic review. *J Dent*. 2013;41:9-16. <https://doi.org/10.1016/j.jdent.2012.10.018>.
  11. Zhou Y, Gao J, Luo L, Wang Y. Does bruxism contribute to dental implant failure? A systematic review and meta-analysis. *Clin Implant Dent Relat Res*. 2016;18:410-420. <https://doi.org/10.1111/cid.12300>.
  12. Dawson PE. *Functional occlusion : from TMJ to smile design*. Edinburgh: Elsevier Mosby; 2006.
  13. Okeson JP. *Management of temporomandibular disorders and occlusion*. 7th ed. St. Louis, Mo.: Elsevier/Mosby; 2013.
  14. Pan W, Yang L, Li J, et al. Traumatic occlusion aggravates bone loss during periodontitis and activates Hippo-YAP pathway. *Journal of Clinical Periodontology*. 2019;46:438-447. doi: <https://doi.org/10.1111/jcpe.13065>.
  15. Passanezi E, Sant'Ana ACP. Role of occlusion in periodontal disease. *Periodontol 2000*. 2019;79:129-150. <https://doi.org/10.1111/prd.12251>.
  16. Forrester SE, Presswood RG, Toy AC, Pain MT. Occlusal measurement method can affect SEMG activity during occlusion. *J Oral Rehabil*. 2011;38:655-660. <https://doi.org/10.1111/j.1365-2842.2011.02205.x>.
  17. Mitchem JA, Katona TR, Moser EAS. Does the presence of an occlusal indicator product affect the contact forces between full dentitions? *J Oral Rehabil*. 2017;44:791-799. <https://doi.org/10.1111/joor.12543>.
  18. Mitchem JA, Katona TR, Moser EAS. Response to letter to the editor: "Does the presence of an occlusal indicator product affect the contact forces between full dentitions?". *J Oral Rehabil*. 2018;45:574. <https://doi.org/10.1111/joor.12652>.
  19. Carey JP, Craig M, Kerstein RB, Radke J. Determining a relationship between applied occlusal load and articulating paper mark area. *Open Dent J*. 2007;1:1-7. <https://doi.org/10.2174/1874210600701010001>.
  20. Kerstein RB. Subjective interpretation pitfalls with paper markings. *Dentistry Today*. 2017.
  21. Koos B, Godt A, Schille C, Göz G. Precision of an instrumentation-based method of analyzing occlusion and its resulting distribution of forces in the dental arch. *Journal of Orofacial Orthopedics / Fortschritte der Kieferorthopädie*. 2010;71:403-410. <https://doi.org/10.1007/s00056-010-1023-7>.

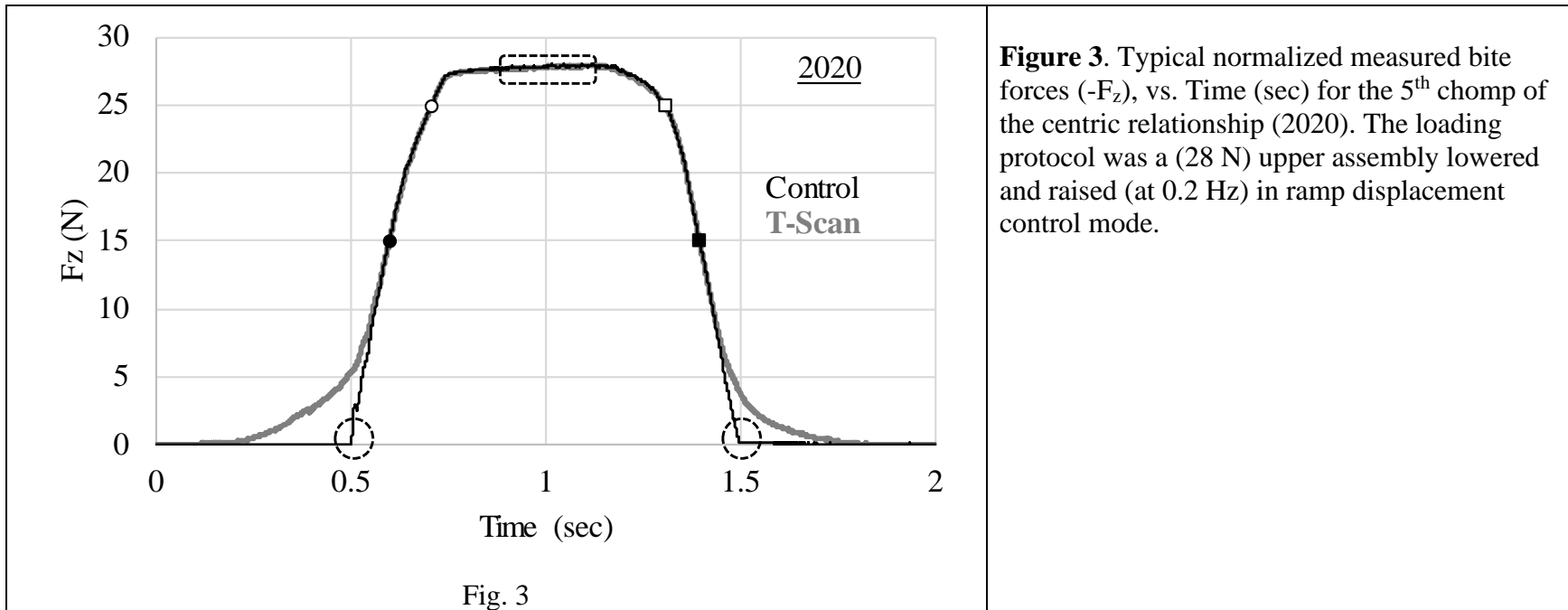
22. Kerstein R, Radke J. In-vitro consistency testing of the T-Scan 10 relative force measurement system. *Soft Computing*. 2022;4:47.
23. Cerna M, Ferreira R, Zaror C, Navarro P, Sandoval P. Validity and reliability of the T-Scan®III for measuring force under laboratory conditions. *J Oral Rehabil*. 2015;42:544-551. doi: <https://doi.org/10.1111/joor.12284>.
24. da Silva Martins MJ, Caramelo FJ, Ramalho da Fonseca JA, Gomes Nicolau PM. In vitro study on the sensibility and reproducibility of the new T-Scan®III HD system. *Revista Portuguesa de Estomatologia, Medicina Dentária e Cirurgia Maxilofacial*. 2014;55:14-22. doi: <https://doi.org/10.1016/j.rpemd.2014.01.001>.
25. Sutter B, Radke J. Letter to the Editor regarding “Does the presence of an occlusal indicator product affect the contact forces between full dentitions?” by Mitchem, Katona and Moser. *J Oral Rehabil*. 2018;45:571-573. <https://doi.org/10.1111/joor.12631>.
26. Kerstein RB, Lowe M, Harty M, Radke J. A force reproduction analysis of two recording sensors of a computerized occlusal analysis system. *Cranio*. 2006;24:15-24.10.1179/crn.2006.004.
27. Beninati CJ, Katona TR. The combined effects of salivas and occlusal indicators on occlusal contact forces. *J Oral Rehabil*. 2019;46:468-474. <https://doi.org/10.1111/joor.12772>.
28. Helms RB, Katona TR, Eckert GJ. Do occlusal contact detection products alter the occlusion? *J Oral Rehabil*. 2012;39:357-363. <https://doi.org/10.1111/j.1365-2842.2011.02277.x>.
29. Thompson JP, Katona TR, Eckert GJ. The significance of loading profile on the occlusion mechanics of a viscoelastic periodontal ligament analogue-supported tooth. *IUPUI ScholarWorks*. 2020. Permanent Link: <https://hdl.handle.net/1805/30052>.
30. Ahuja S. *Immediate effect of complete denture occlusal errors on masticatory muscle EMG activity in denture wearers: A pilot study*, University of Tennessee Health Science Center; 2009. <http://dx.doi.org/10.21007/etd.cghs.2009.0009>.



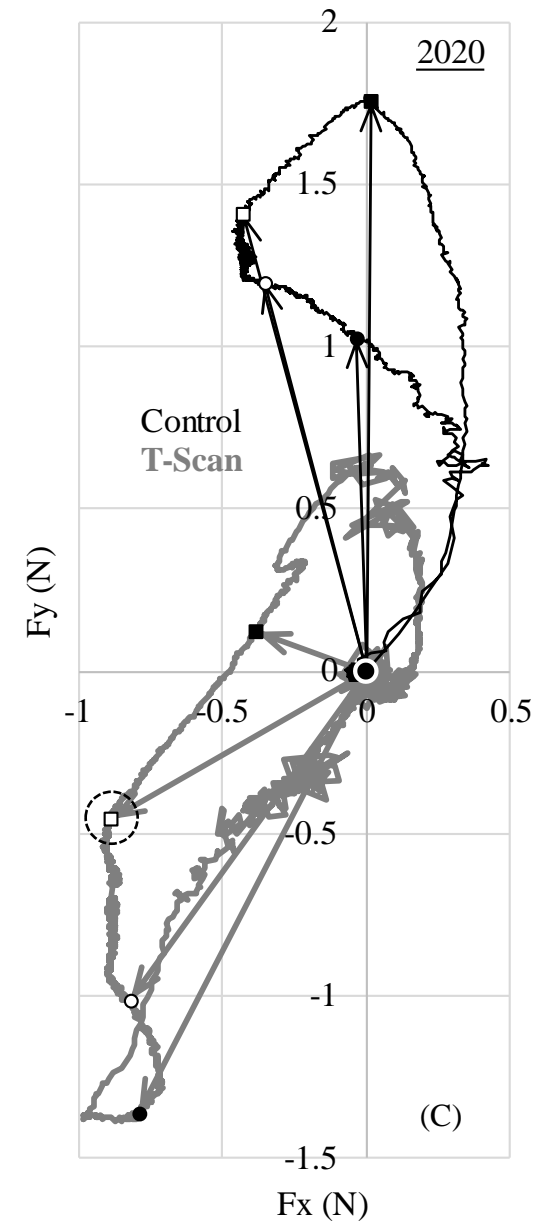
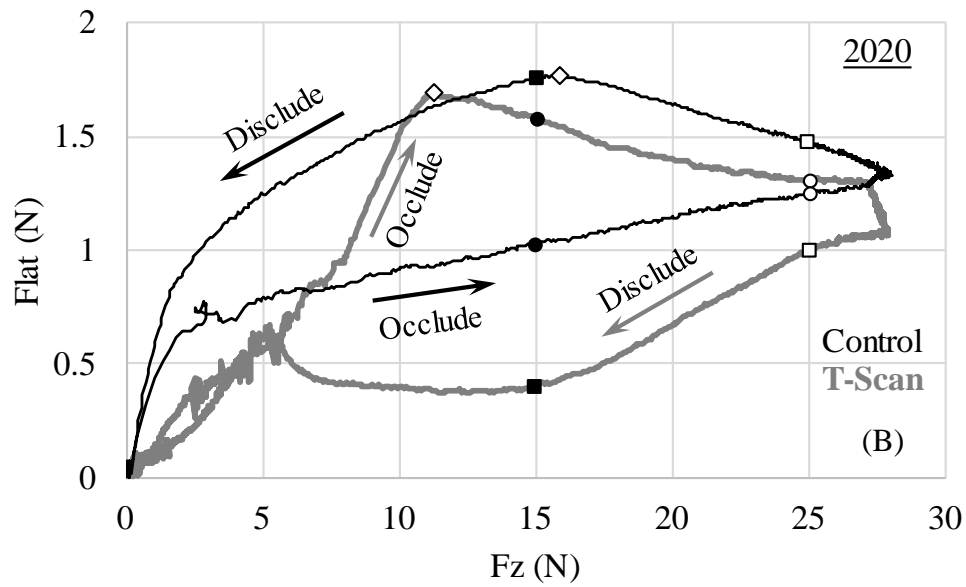
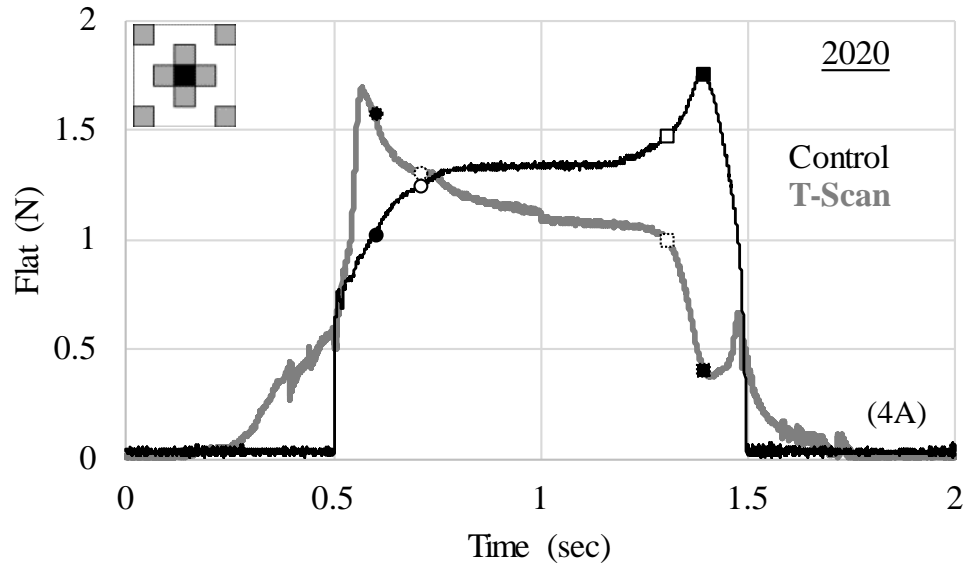
**Figure 1.** (A) The testing apparatus (B) Schematic of denture tooth mounted in its holder and attached to the load cell. (Also shown is the coordinate system.) The maxillary tooth is in a similar holder.

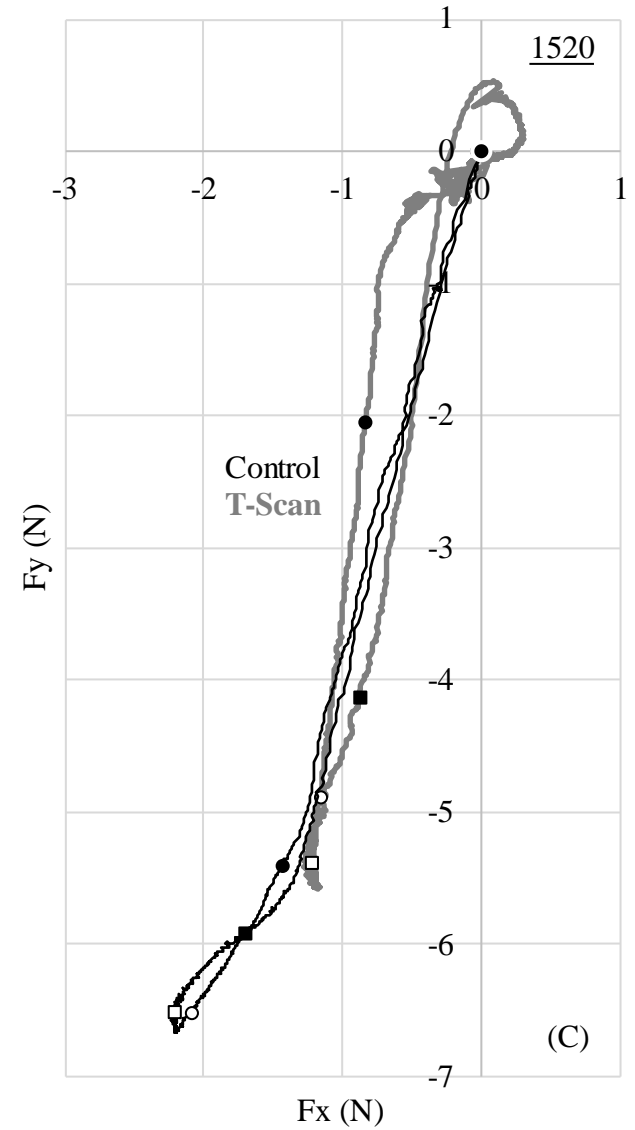
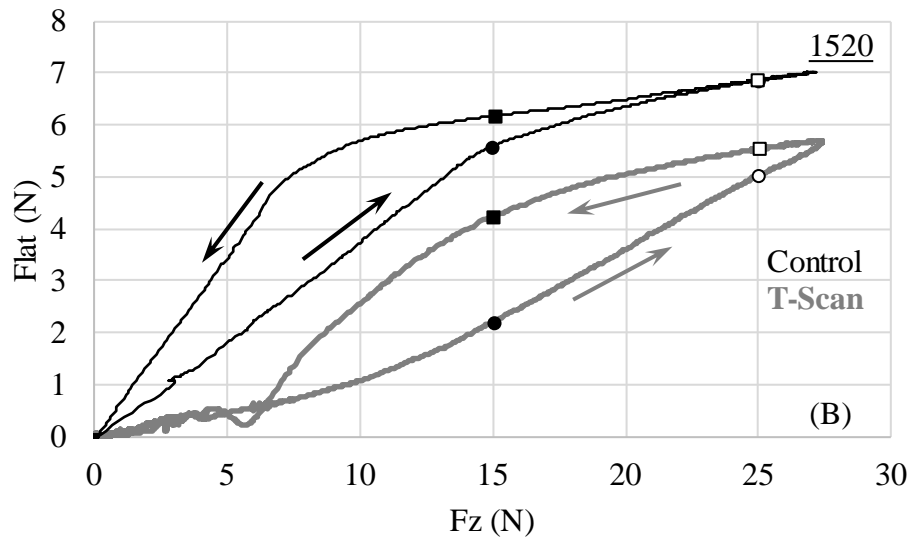
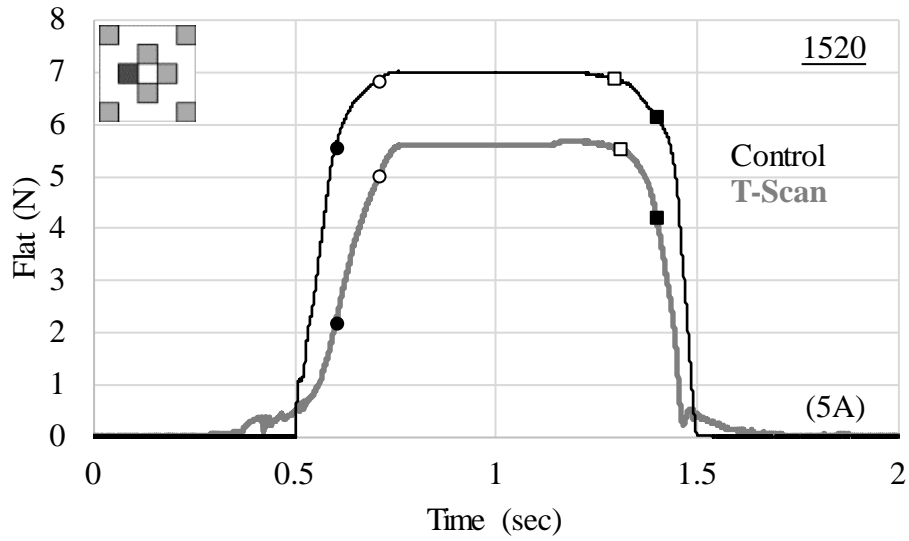


**Figure 2.** Layout showing the 21 positions of the lower assembly that were tested. The nomenclature is in the form xxxy where xx and yy correspond to the distances, in mm x 100, from centric, 2020. Data of the underlined configurations are used to illustrate results in **Figures 4 - 8**.

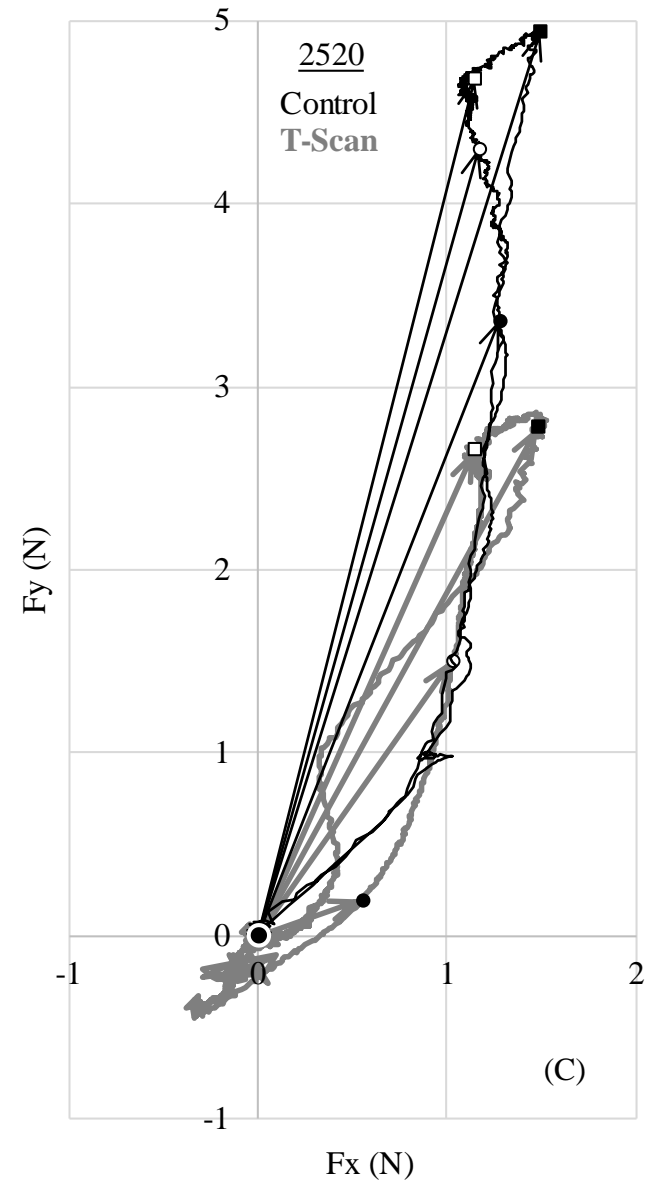
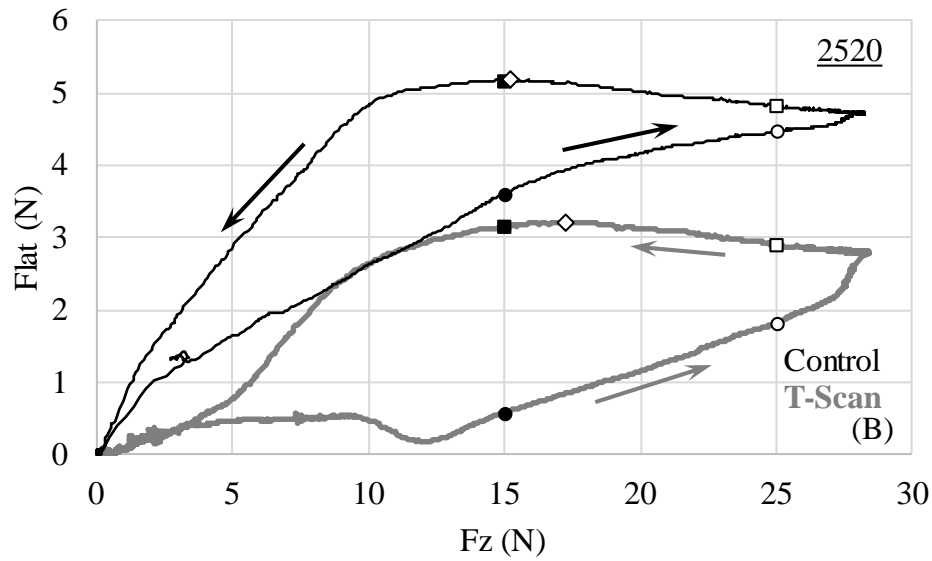
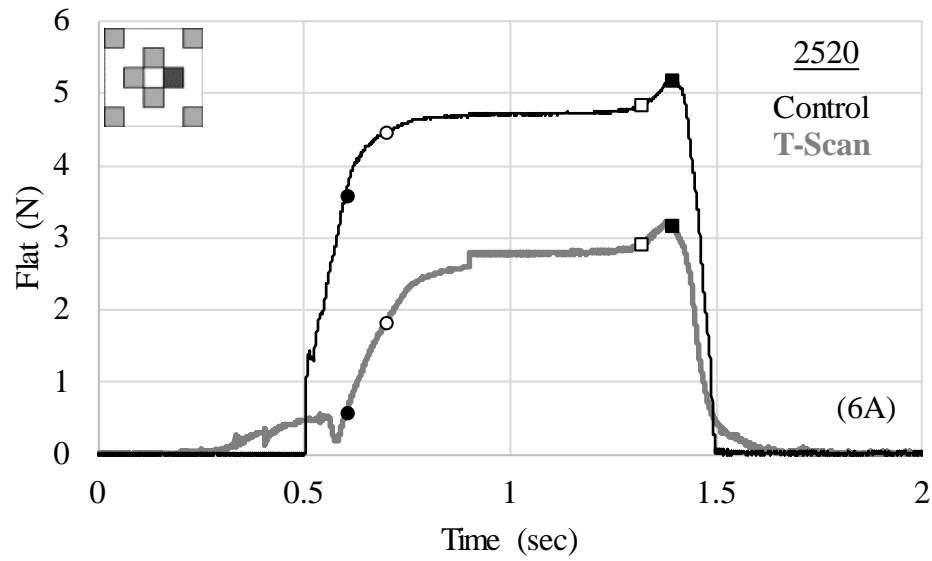


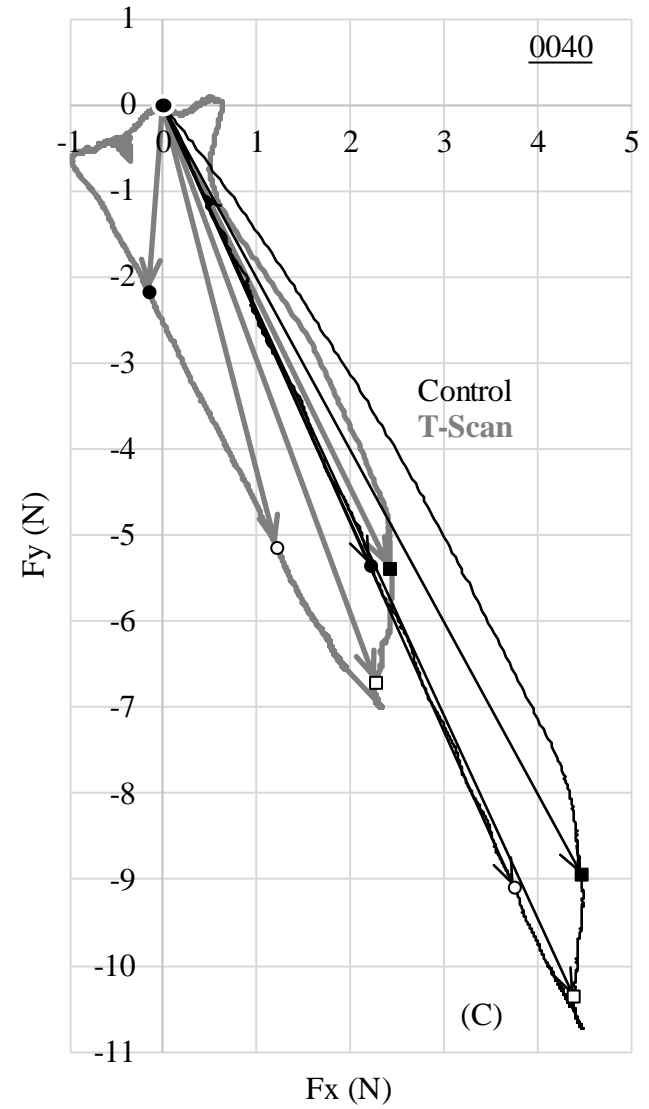
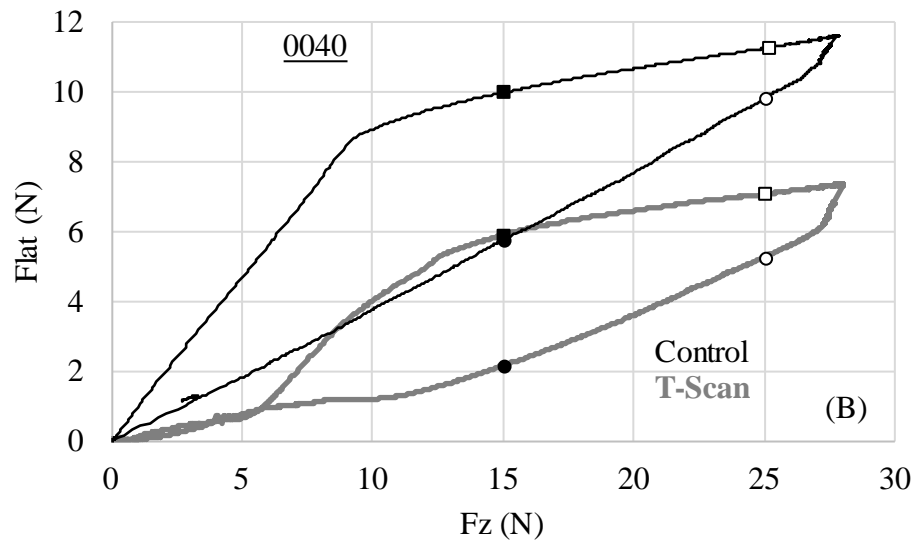
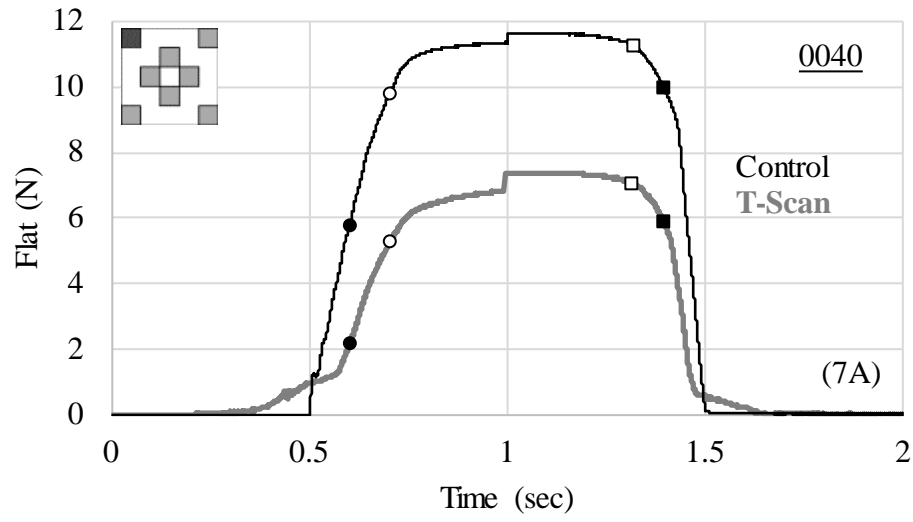
**Figures 4 - 8.** Results for 2020 (Centric), 1520, 2520 (2 of the closest position, 0.05 mm, to Centric), 0040 and 0000 (2 of the furthest position, 0.283 mm, from Centric), respectively, in **Figures 4, 5, 6, 7** and **8**.  $F_{lat}$  is graphed against Time in **(A)**,  $F_{lat}$  vs.  $F_z$  in **(B)** and  $F_y$  vs.  $F_x$  in **(C)**. The symbols ( $\bullet$ ,  $\blacksquare$ ,  $\circ$  and  $\square$ ) are the same as in **Figure 3**. In **Figures 4B** and **6B**, the  $\diamond$  indicate the peak values of  $F_{lat}$ .

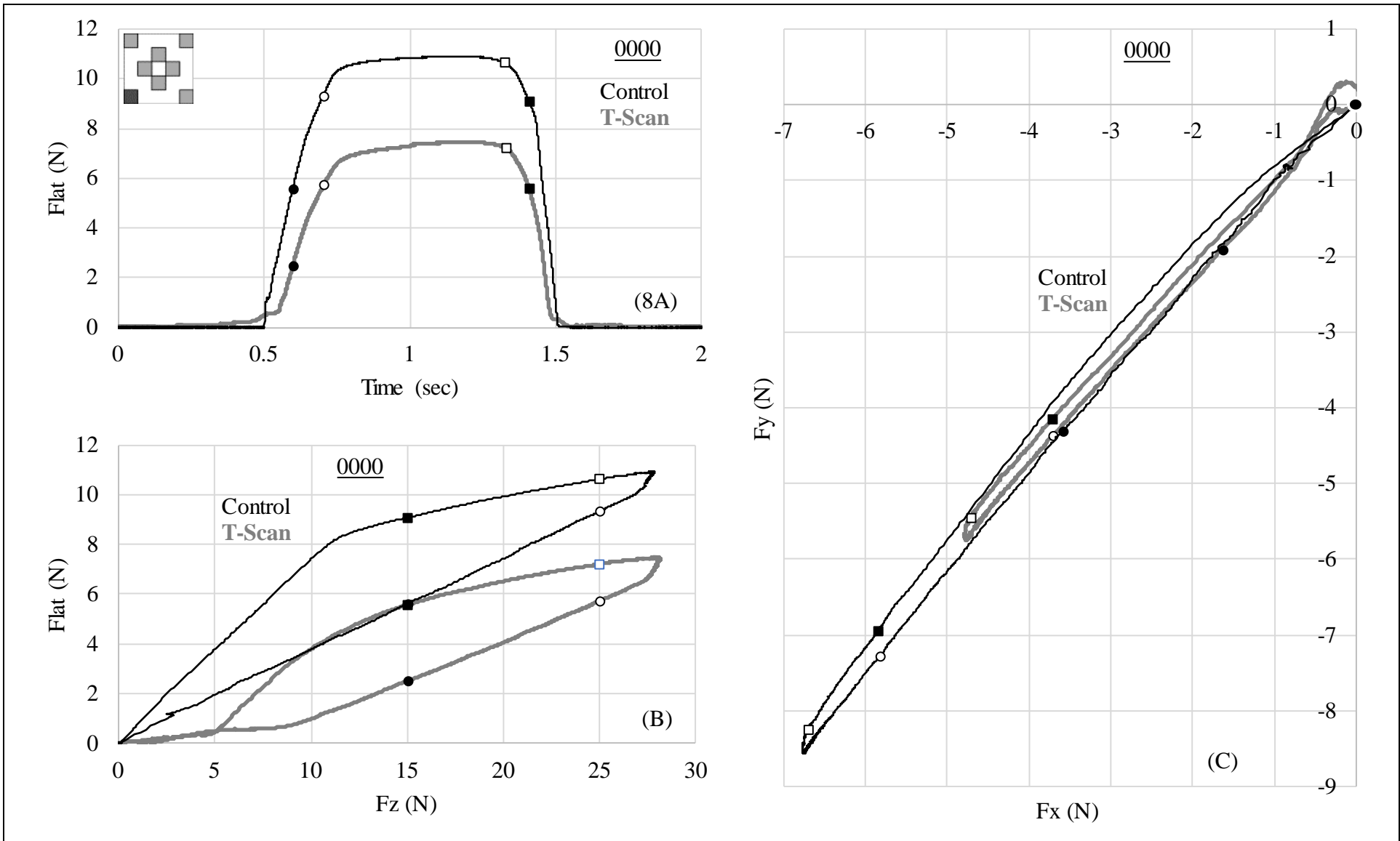












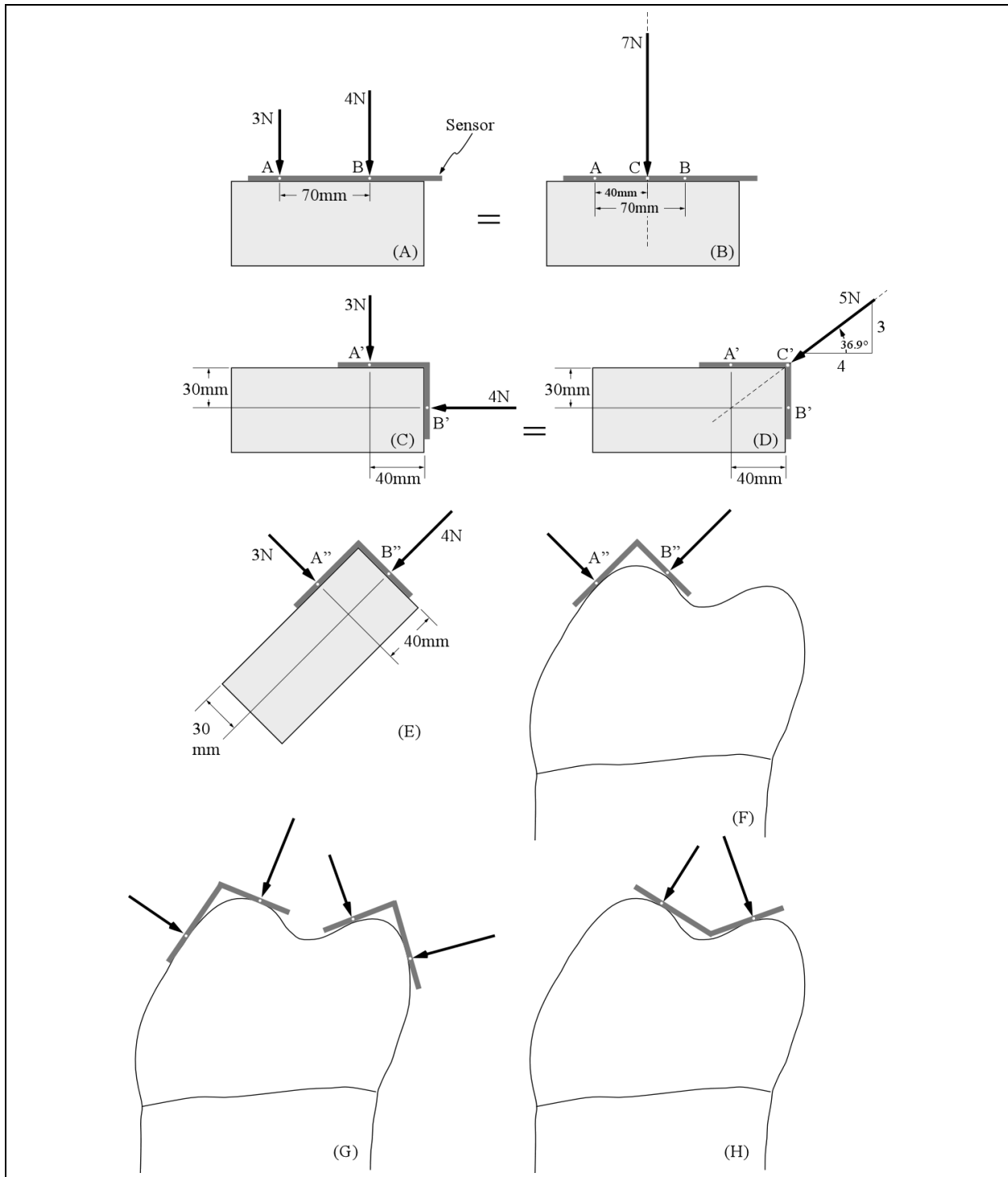


**Figure 9.** Points A and (A' and A'') and B (B' and B'') are 2 specific locations, 70 mm from each other, on the sensor. In all drawings, the contact forces are 3N and 4N, respectively, on points A (A' and A'') and B (B' and B''). **(A)** Flat-plane occlusion and **(B)** its equivalent system. **(C)** Deformed sensor and **(D)** its equivalent system. **(E)** Rotated structure **(F)** superimposed on a contacting cusp. **(G) – (H)** Examples of configurations that T-Scan does not distinguish from the flat-plane occlusion depicted in **(A)**.

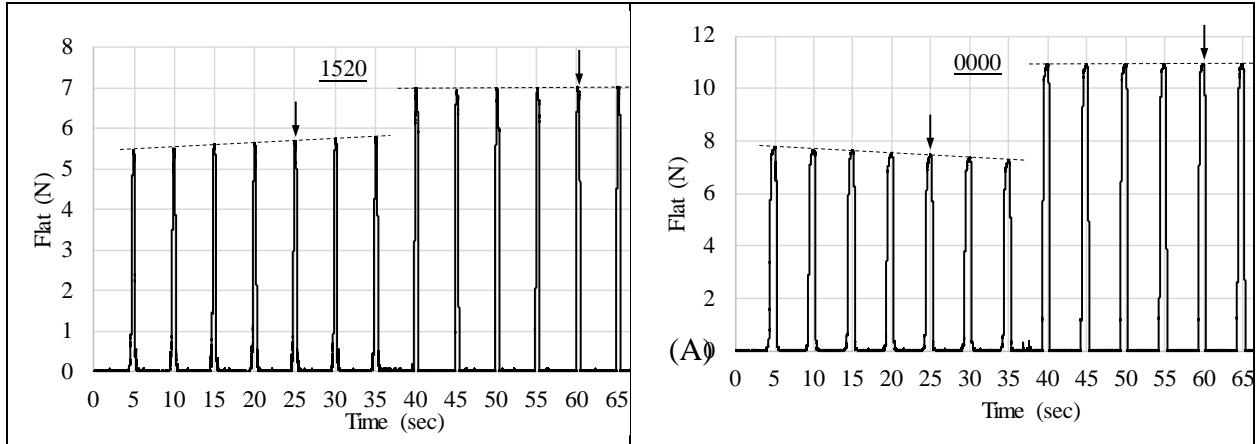


**Figure 10.**  $F_{lat}$  vs. Time for occlusal relationships (A) 1520 and (B) 0000. The 7 chomps with T-Scan and control occur from 5 to 35 seconds and from 40 to 70 seconds, respectively. In these examples, the readings with T-Scan do not stabilize at the 5<sup>th</sup> chomp (arrows), increasing in one instance while decreasing in the other.

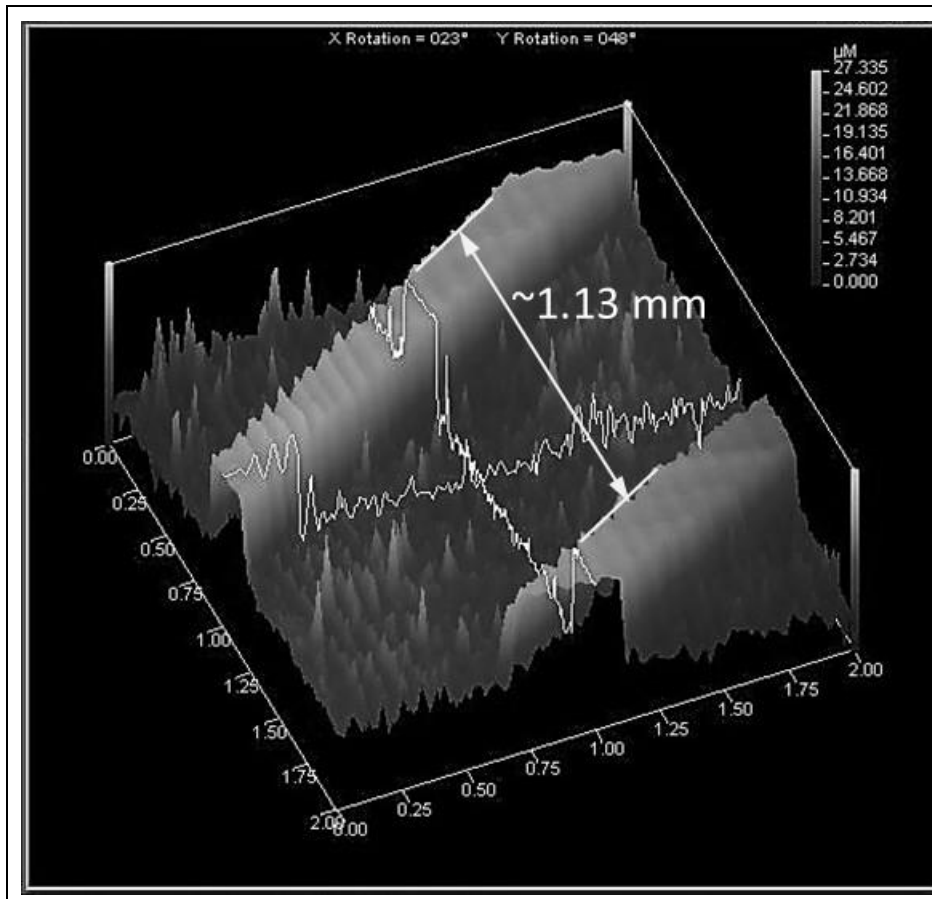


**Figure 11.** Profilometer measurements of sensor surface.